Talanta Open 4 (2021) 100062

Contents lists available at ScienceDirect

Talanta Open

journal homepage: www.sciencedirect.com/journal/talanta-open

# Moldable capillary suppressor for open tubular ion chromatography based on a polymeric ion exchanger.

Fereshteh Maleki [1], Bikash Chouhan [1], Charles P. Shelor, Purnendu K. Dasgupta [*]

*Department of Chemistry and Biochemistry, University of Texas at Arlington, Arlington, Texas, 76019-0065, USA*

ARTICLE INFO

*Keywords:*
Suppressor bleed
Mass spectral background
Moldable cation exchanger
Open tubular suppressor

ABSTRACT

We successfully fabricated 45 μm bore microchannels in PVA-Poly(styrenesulfonate) cation exchange polymers. by casting aqueous prepolymer mixtures around fine tungsten wire mandrels, curing, crosslinking by thermal annealing, and subsequently removing the microwire. This was then used as a chemically regenerated micro-suppressor (with a cleaner MS background than its commercial macro counterparts) for open tubular ion chromatography, with an integrated tubular conductivity cell, tested to backpressures up to 600 psi. The overall system permits detection limits for common inorganic ions in the low μg/L levels with a 4-nL injection, isocratic elution and regeneration with poly(styrene sulfonic acid).

## 1. Introduction

Conductivity is a universal trait of ions in solution. As such, it is the detection mode of choice in ion chromatography (IC). In IC, the mobile phase is obligatorily an ionic eluent, typically of a concentration orders of magnitude greater than those of the analytes of interest. Detecting trace ionic analytes in such a highly conductive background would be impossible; this problem was solved by eluent *suppression* [1].In anion chromatography, the *suppressor* is a proton exchange device that exchanges all influent cations for $H^+$. Placed before a conductivity detector, it converts an alkali hydroxide or the salt of a weak acid (e.g., Na-borate) used as eluent to pure water or weakly conducting boric acid, respectively while analytes like $Cl^-$, $NO_3^-$, $SO_4^{2-}$ etc. enter the detector as highly conductive corresponding acids. From their original packed resin bed incarnation, suppressors have long adopted continuously regenerated membrane-based forms. A recent review covers this, along with other analytical uses of ion exchange membranes [2], but of course they will continue to evolve [3].

From reduced sample and eluent consumption to a smaller footprint, miniaturization has many benefits, IC is no exception. The first microscale suppressed IC utilized a 0.19 mm i.d. packed column coupled to a thermally stretched Nafion® perfluorosulfonate tube with active dimensions of 200 μm i.d. and 10 mm length as suppressor [4]. Others later used a 11 mm long ~100 μm i.d. (estimated, dry i.d. given as 80 μm) tubular Nafion suppressor [5] or a 19 mm long 50 μm i.d. radiation-grafted sulfonated PTFE tube [6] with 180 μm i.d. packed columns.

Capillary IC was first reviewed in 2004 [7]. Since that time the alternate use of two packed capillary suppressors was advocated for use with larger (320 μm i.d.) capillary columns [8]. However, contemporary interest has been on open tubular (OT) IC, which has been recently reviewed [9,10]. Because of much smaller band volumes, making a small enough suppressor is a much greater challenge for OT columns than with packed columns. The first OTIC suppressor was fabricated by repeated coating of a 50 μm Pt-wire mandrel placed between two 75 μm i.d. capillaries with a colloidal solution of Nafion [8,11].] The suppressor suffered from poor adhesion of the membrane to the column.

The mandrel approach was continued by this group by forming a polymer around the mandrel and functionalizing the polymer further into an ion exchanger [12,13]. However, these suppressors were used with columns too large to be practical. The first practical OTIC suppressor was electrodialytic and was used successfully with 20-30 μm i.d. columns [14]. This device contained two 0.45 mm φ drilled parallel regenerant channels for electrode placement bracketing an eluent channel in a block of Nafion. The eluent channel was made by puncturing the solvent-swollen polymer with a 0.3 mm φ needle; the polymer is not physically removed, but a *crack* is made. The honed end of a capillary column and a similar tapered exit tube were inserted into this channel from opposite sides, leaving a suppression gap of 400-1100 μm. The close placement prevents the crack from sealing itself. With an

* Corresponding author.
*E-mail address:* dasgupta@uta.edu (P.K. Dasgupta).
[1] These two authors share equal credit

https://doi.org/10.1016/j.talo.2021.100062
Received 15 July 2021; Received in revised form 10 August 2021; Accepted 10 August 2021
Available online 12 August 2021

applied electric field, such a device can provide more than adequate suppression capacity, up to 100 mM KOH @ 100 nL/min and excellent signal-to-noise (S/N) ratio for both isocratic and gradient elution modes. The design has several disadvantages, however: (a) The *cracks* do not translate to reproducible channels from one device to another, (b) When flow is stopped, especially for an extended period and then restarted, the crack does not necessarily regain the original dimension; in a constant pressure flow system this change in restriction undesirably affects the overall flow rate, and (c) Nafion blocks of necessary dimensions are not commercially available.

Such a device can also be used with chemical regeneration, where only the eluent channel is needed [15]. While the suppression gap is $\sim<$ 1 mm, the overall depth of the channel must be several mm to securely hold the column and the exit tube. Laser drilling is not possible because of thermal decomposition of ion exchange polymers (IEPs). Because of limited flute lengths of mechanical drills of diameters <150 μm, drilling a ~ 5 mm long hole through a polymer block is not possible with any smaller drill. Such drilled channels do not change backpressure over time but even over sub-mm lengths, the dispersion of bands from a 20-25 μm i.d. column is very noticeable. We have recently described a high-capacity IEP with attractive properties, including the ability to be molded around/on existing structures [16]. Such a material can allow two previously advanced concepts of (i) having a column and an exit tube with a wire mandrel inserted between them, and casting an IEP around the mandrel, and (ii) having a predrilled IEP block and inserting the column and the exit tube into it, to be combined. As mentioned, the former has problems of a cast IEP adhering to a capillary exterior upon wetting and the second has the difficulty of drilling a long enough hole small enough in diameter. If an IEP block is preformed around a microwire mandrel, which can then be removed, honed column and exit tube ends can be forcibly inserted into the premade channel making leakproof connections and leaving a small suppression gap of desired length. The fabrication and characterization of such a device is described in this paper, along with a tubular metal capillary functioning as the suppressor exit, as well as the first conductivity detection electrode in contact with the suppressed effluent. The terminal electrode, of a similar metal capillary, is placed only ~100 μm from the first, joined by an insulating sleeve.

## 2. Experimental section

### 2.1. Reagents and materials

Poly(vinyl alcohol) (PVA, 98-99% hydrolyzed, 88-97 kDa, alfa.com); sodium p-styrenesulfonate hydrate (SSNa, 93.0%, tciamerica.com), ferrous ammonium sulfate heptahydrate (avantorsciences.com), hydrogen peroxide (30%, fishersci.com), and acetic acid (ACS grade, us.VWR.com) were obtained as indicated.

### 2.2. Capillary suppressor. IEP synthesis

Details of making this class of polymers have been previously given [16]. To make the specific composition used here, Fenton's reagent (100 μL 3% w/v $H_2O_2$ freshly added to 100 μL 1 mM $Fe(NH_4)_2(SO_4)_2$) as initiator was added to 32 mL of a mixture of 75% by weight PVA and 25% by weight sodium styrenesulfonate (SS) and mixed well. Note that the (pre)polymer solution was prepared in the sodium ($Na^+$) form.

### 2.3. IEP Microchannel fabrication

The procedure for casting the (pre)polymer solution around a tungsten wire mandrel was previously described [16]. In the present work, up to three parallel microchannels, each 30-35 mm long, were simultaneously prepared in a single IEP block. As actual suppressors require only $\lessapprox$ 8 mm lengths, multiple usable units could be sliced and diced from each batch. A 35 mm diameter plastic petri dish is used as the mold. Three diametrically opposed small holes, 5 mm apart, were drilled on the walls of the dish, ~2 mm from the bottom, and 3 strands of tungsten wire, 15-50 μm in dia., were strung across and fixed taut in place with a drop of hot-melt adhesive each at the entry and exit points (See Figure S1 in Supplementary Information (SI)). The prepolymer solution was poured over the assembly to a height of 2+ mm above the wires; and allowed to polymerize at room temperature for 5-7 days in a vibration/dust-free environment. After the dry polymer was formed, the hot glue was removed, and the assembly annealed for 24 h at 120 °C. Next, the polymer disks with the wires still imbedded therein were repeatedly treated with 0.1 M $H_2SO_4$ ($\geq$ 2 h each time, at least 10 times) to convert the material to the proton form. After washing thoroughly with water, the disk was annealed again at 120 °C but only for 3 hours. In the presence of the strongly acidic sulfonic acid, the PVA dehydrates and crosslinks, forming poly(ene)s and turning dark brown. Over-annealing in the acid form makes the polymer brittle while under-annealing may lead to leaching of styrenesulfonate. Next, the polymer disks were submerged in DI water for 4-7 days; upon hydration the polymer expands sufficiently to detach from the wires, which could now be removed. Removing the wires mechanically by simply pulling on them does become more difficult with smaller diameter wires but it is possible for the entire range of wire diameters stated. Except as stated, data reported here rely on devices made with 35 μm wires.

### 2.4. Post-fabrication steps

Each suppressor block is cut to a size of ~2 mm thick, 4 mm wide, and 8 mm long. High-resolution digital microscopy (VHX-5000, www.keyence.com) was used for dimensional characterization. Initial examination, however, showed a thin layer of black particles in the channel, possibly originating from the black oxide-coated exterior of the tungsten wires used. Use without further cleaning led to discernible noise in the conductivity signal, likely due to sporadic dissolution or dislodgement of such particles. Each device was therefore washed (using 365 μm silica capillaries forcibly inserted into the channels for liquid I/O) for a prolonged period (4 days, 2 μL/min) with a micropump capable of high pressures. The initial registered pressure of 115 psi decreased to ~30 psi after washing. A clear and clean channel was microscopically observed after washing it further with 1 M $H_2SO_4$ pneumatically @ ~200 nL/min for 3 h.

### 2.5. Leaching studies. Suppressed background conductance and mass spectrometry (MS)

The background conductance of the suppressor effluent is an indication of any ionic monomer/oligomer leaching from the suppressor. Rather than pure water, we used electrogenerated KOH as the influent. Contamination of stored water with $CO_2$ is impossible to avoid; electrogenerated KOH produces a lower suppressed conductance than a water influent, and also reflects more realistic in-use suppressor conditions. The test arrangement is shown in Figure S2. An ICS-2000 pump delivers water @ 100-400 μL/min through a KOH eluent generator, and a 2 × 250 mm AS-19 IC column. The flow was split after the column by a tee between the OT-scale suppressor developed in this work (hereinafter called a μsuppressor) and the commercial macrosuppressor (2-mm ERS-500, all above from www.thermofisher.com). A PEEK restrictor tube (25/360 μm i.d./o.d., 1.52 m long) preceded the μsuppressor. The flow split ratio between the macrosuppressor and μsuppressor was measured to be 227:1. The macrosuppressor effluent conductivity was measured by the ICS-2000 conductivity detector, calibrated with standard KCl.

### 2.6. μSuppressor and μconductivity cell

The μsuppressor was followed by a μconductivity cell, constructed from custom stainless-steel (SS) tubes, 38/150 μm in i.d./o.d. (www.k-tube.com). The basic configuration is similar to that utilizing

hypodermic needle-based conductance cells [17]. The first tubular electrode (~ 8 mm long) was inserted into one end of the IEP microchannel. The free end of the SS tube was then inserted into a short segment of a 150/360 μm i.d./o.d. PEEK tube. The second electrode tube was then inserted into the open end of the PEEK tube until it touched the first electrode (monitored ohmically). The second electrode was then retracted with a rotatory motion until the electrical contact was broken. The honed end of a separation column or other connecting tube was then inserted into the entrance of the suppressor channel leaving a gap of 2.2, 0.7, or 0.4 mm (this is the active suppressor length, microscopically measured, respectively designated μsuppressor A, B, and C), between the column/tube end and the first electrode. See the inset of Fig. 1 for the μsuppressor-detector arrangement. The cell constant, as measured with a standard KCl solution for a number of the μconductivity cells constructed in the above fashion ranged from 60 to 110 $cm^{-1}$. Given the area of the metallic annular face of each electrode is calculated to be $1.65 \times 10^{-2}$ $mm^2$, these cell constants imply the gap between the electrodes to be of the order of 99-182 μm; however, this can be correspondingly larger if the inner surfaces of the tubes play any role.

### 2.7. MS Experiments

Prior to MS experiments, water was pumped through μsuppressor A (active length 2.2 mm) and the macrosuppressor continuously for two weeks to simulate use. Data such as those represented by Fig. 2 were obtained with both water and 0.01% v/v acetic acid as the influent in both suppressor cases at respective flow rates of 5 and 250 μL/min using a syringe pump and a HPLC pump. Water and HOAc respectively simulated background conditions, and that of an acidic analyte elution. In all cases, 60 30-s long scans with a FWHM resolution of 0.7 amu, spanning the full 30-1500 m/z range of the instrument, were acquired, averaged, and exported. MS ((Thermo TSQ Quantum Discovery Max) operating conditions are in the supplementary material (SM).

### 2.8. Suppression capacities

The suppression ability of μsuppressor A was tested for 1-16 mM KOH; at flow rates between~440 - 1700 nL/min as preparatory studies for the MS-based leaching experiments (see below). However, both the active length of μsuppressor A and the flow rates used are much larger

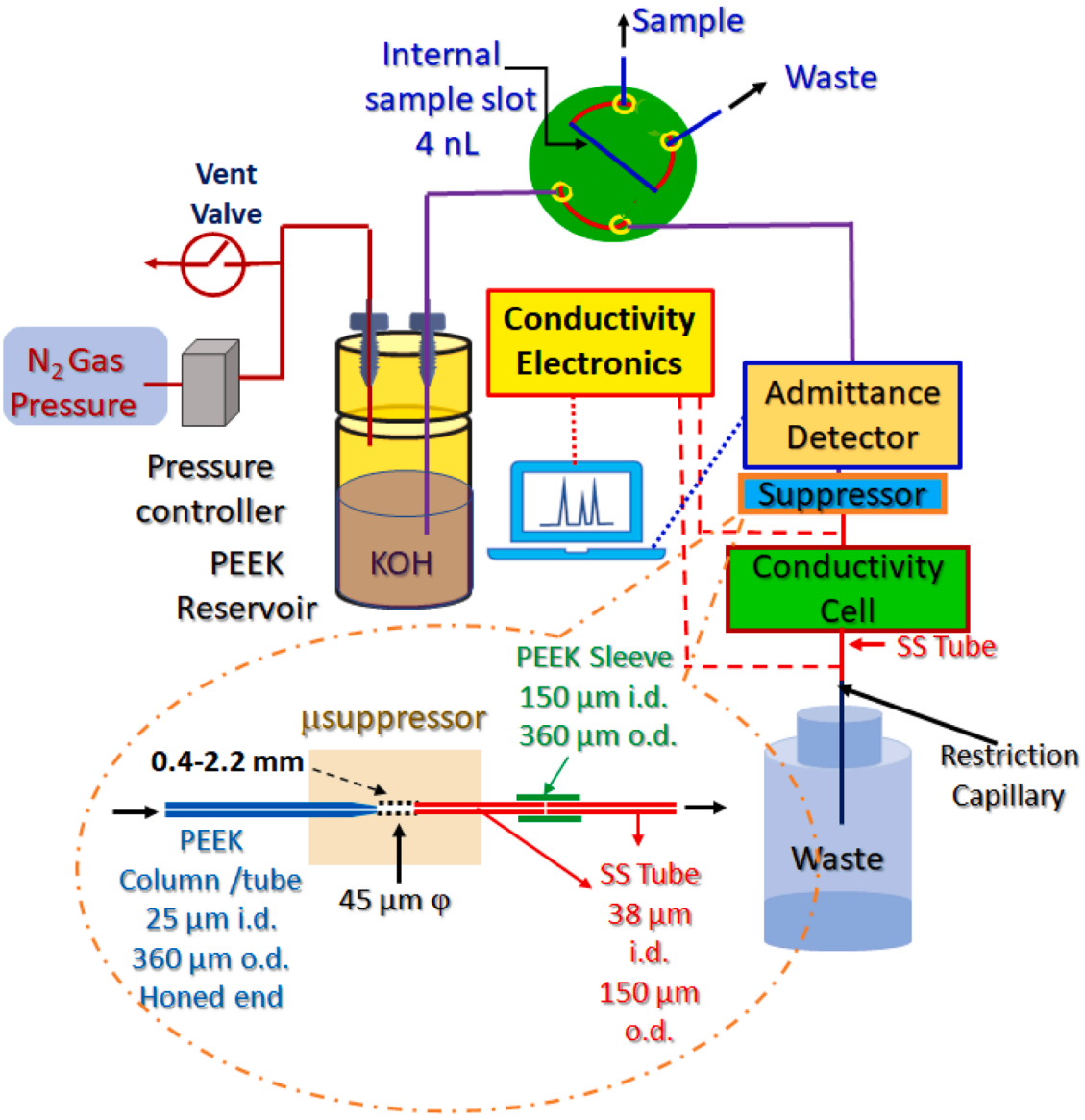


**Fig. 1.** System set up for testing the PVA-SS microchannel suppressor. Chromatograms were also obtained using this arrangement. The admittance detector provides the unsuppressed signal; the post-suppressor conductivity cell connected to its own electronics generates the suppressed signal.

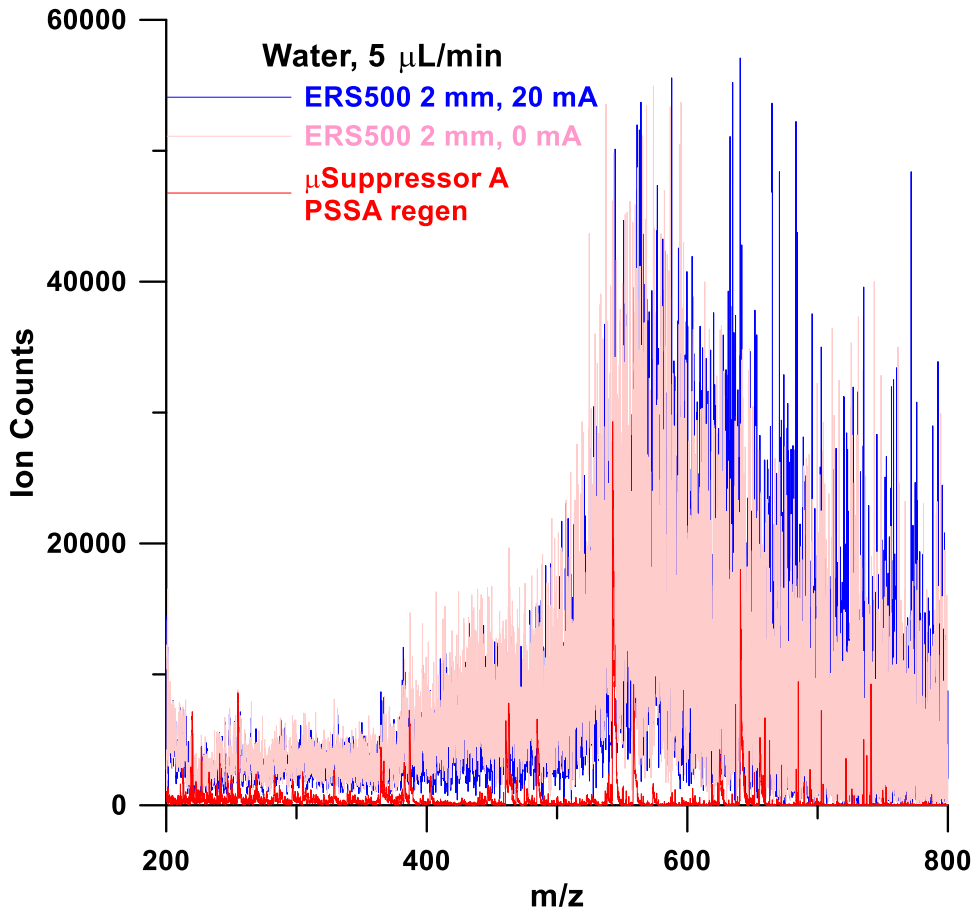


**Fig. 2.** Suppressor MS background counts, water influent. See Figure S7 for data for 0.01% HOAc influent.

than those used in actual OTIC. Therefore, as seen in Fig. 3, suppression capacity experiments were further conducted with μsuppressor B (active length 0.7 mm), operated at a more typical OTIC flow rate of 168 nL/min (column velocity 5.7 mm/s) using electrogenerated KOH eluent from a capillary ICS-5000 system and a split-flow arrangement to generate a step-gradient. Experiments were conducted with 10-20 mM polystyrene sulfonic acid (Av. MW 75 kDa, purified by dialysis (courtesy Diduco AB, Umeå, Sweden) as a stationary regenerant surrounding the μsuppressor.

### 2.9. Chromatographic system

The chromatographic system is illustrated in Fig. 1. A digital pressure controller (P/N 990-005103-100, https://ph.parker.com/us/12051/en/oem-ep-miniature-pressure-controller) provided pneumatic pressure to drive manually prepared KOH as eluent. A solenoid vent valve (Skinner Valve, New Britain, CT) allowed for quick release of pressure when desired. An electrically actuated 4-nL internal loop injector (C74MPKH-4574-.004EH, www.vici.com) was used to inject the sample. PEEK capillaries (25/360 μm i.d./o.d., P/N 1574, www.idex-hs.com) were sulfonated and then coated with AS18 latex (Courtesy Thermo Fisher Scientific) to make an OT anion exchange column [10]. A variable-frequency admittance detector (TraceDec, www.istech.at) was placed on the column immediately before it entered the μsuppressor, which was followed by the μconductivity cell. The system was controlled by a desktop computer with software written in LabView™ in-house [10]. All data were acquired using a programmable system on chip, PSoC5LP (CY8CKIT-059, www.cypress.com) @ 183 Hz.

## 3. Results and discussion

### 3.1. Leaching from suppressor membranes

Degradation of IEPs occurring over time lead to loss of ionic functional groups [18–21]. Only significant loss of such groups will be registered by an elevated conductance background; given the low conductance background attained in routine IC, such major leaching does not occur in commercial suppressors. However, larger molecular weight ions, which do not necessarily have high mobility in solution, may not contribute much to background conductance and still present a significant and undesirable background in mass spectrometry. We have previously reported ESI-MS data for several commercial suppressors for anion chromatography [22], albeit presently available suppressors are many and contain a great variety of ion exchange membranes and screens; it was not possible to test all of them. However, the devices tested uniformly showed most of the ion current is due to peaks present in 400-800 m/z range and not surprisingly, by far the greater amount of signal was seen in the negative ion mode; anion suppressors contain negatively charged cation exchange material. The nature of leaching from the new μsuppressors is therefore of interest both qualitatively and quantitatively. However, there is some difficulty in a quantitative comparison with macrosuppressors because dimensions and use conditions are so different. Presently described μsuppressor A has a residence volume of $3.5 \times 10^{-3}$ μL, and the typical OTIC flow rate is 0.15 μL/min; the 2 mm ERS500 has an estimated internal volume of 15 μL and the typical flow rate is 250 μL/min. Unfortunately, MS examination of the effluent under these operational conditions is not possible for the μsuppressor; the present MS instrument will reliably operate only at flow rates $\geq$ 5 μL/min. As a first approximation, the mass of the leachate in

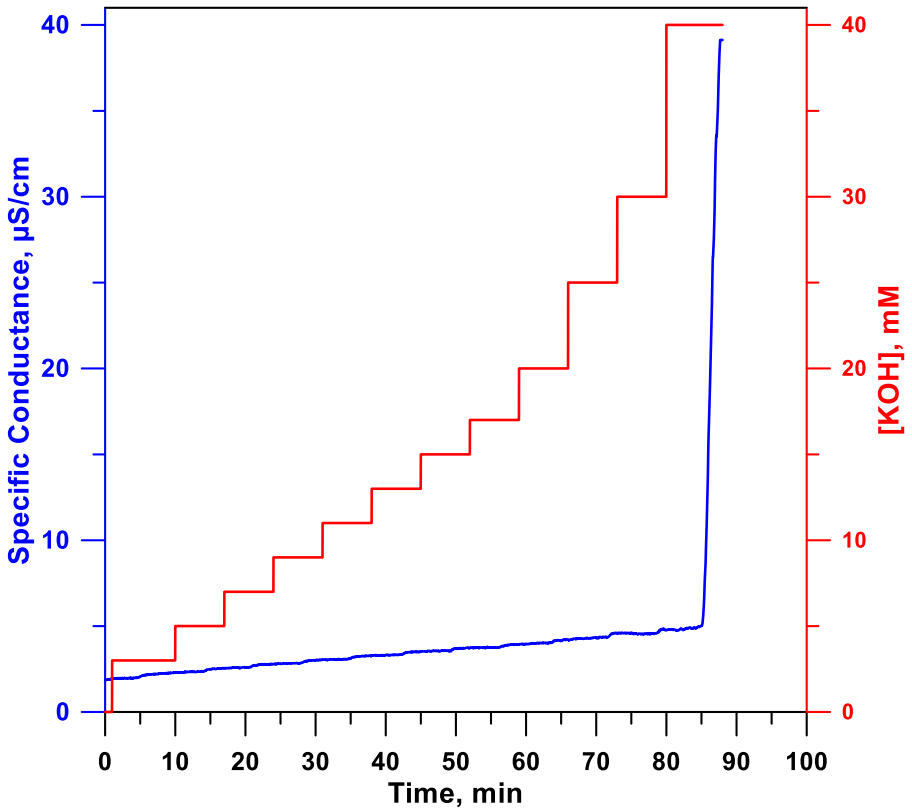


**Fig. 3.** Suppressed background conductance exhibited by µsuppressor B (0.7 mm active length) at a flow rate of 168 nL/min as KOH concentration is changed stepwise.

the effluent should be independent of the flow rate. If the MS would behave as a strictly mass-sensitive detector, then the MS output should not markedly differ if a given suppressor is operated at two different flow rates and the entire effluent is seen by the MS, within the limitation that nebulization and ionization efficiency decreases to some degree with increasing flow rates. On the other hand, if the impurity ions originate not in the suppressor but the influent fluid itself, the signal will increase with increasing flow rate. Raw ion chromatograms for pumping (a) DI water and (b) 0.01% HOAc pumped into the MS at 5 and 250 µL/min (i) directly (ii) through the ERS-500 suppressor with 0 and 20 mA drive currents are shown in Figure S3 and S4. It will be readily seen that the impurities in the influent water blank are essentially confined to the m/z ≤200 range. Figure S5 is more instructive in that it plots the ratios of the cumulative ion counts at the two different flow rates in 7 different mass ranges for pure water as influent (the data are available in Table S1) as a function of blank water counts. Except for the m/z ≤200 range, in all other cases the ion counts for the suppressor effluent at the 50x different flow rates are quite comparable, including the m/z 200-800 range, where much of the non-blank signal originates. The same is observed for the HOAc influent, notably that the total ion counts in the m/z 200-800 region are comparable at the two flow rates (Figure S6, Table S2).

With the above in mind, we compared the MS response to the µsuppressor A and ERS-500 effluents, both at 5 µL/min. The results are shown in Fig. 2 and Figure S7 for water and HOAc influents, respectively; the difference is notable. Indeed, Figure S8 shows that the overwhelming majority of the peaks observed for µsuppressor A are also present in the blank water.

### 3.2. Background conductance measurements

The suppressed background conductance (SBC) from µsuppressor A remained between 1.2-2.0 µS/cm for 1-16 mM KOH concentrations @ 440 nL/min, with a linear $r^2$ value of 0.9890 and an intercept of 1.25 µS/cm, suggesting complete suppression (Figure S9). Suppression appears to be complete also at 845 nL/min, albeit the SBC was slightly higher at 1.7-4.7 µS/cm. However, at 1300 and 1700 µL/min, suppression capacity was clearly exhausted at some point between 8 - 12 mM and 4 – 8 mM, respectively. The maximum mass flux with demonstrated complete suppression would thus be 13.5 neq/min, corresponding to 43.4 neq/(mm$^2$.min) for the 0.311 mm$^2$ available membrane area. The macrosuppressor, with a total membrane area of ~740 mm$^2$ (K. Srinivasan, Thermo Fisher Scientific, personal communication, June, 2021) specifies a maximum suppression capacity of 200 mM KOH @ 0.25 mL/min, that translates to a comparable 67.6 neq/(mm$^2$.min), which, however, is accomplished in the presence of an electric field. Also notable in the data in Figure S9, is that at low eluent concentrations (≤2 mM), where the eluent is completely suppressed regardless of the flow rate, the µsuppressor SBC actually increases with increasing flow rate, opposite of what will be expected if conductive monomers were significantly leaching from the suppressor at a constant rate.

As previously stated, µsuppressor A has too large an active length and tested flow rates were larger than presently used OTIC systems. µsuppressor B (0.7 mm gap) was therefore tested at a fixed flow rate of 168 nL/min, typical of present OTIC use, while the KOH concentration was stepped through 0, 3, 5, 7, 9, 11, 13, 15, 17, 20, 25, 30, and 40 mM, with 10 min dwell time at each concentration. Fig. 3 shows the SBC data as a function of time. The data indicates that the device can suppress up to 30 mM KOH at this flow rate. Although this observed capacity may be regenerant concentration/flow limited, we did not presently explore this further as OTIC columns require a much lower eluent concentration to get the same retention factor. It has been shown that packed and OT columns based on the same latex particle not only have the same selectivity but the exact retention factors at the same eluent concentration are proportional to the stationary phase capacity per unit eluent volume in the column, termed $\gamma_{iex}$ [23]. The $\gamma_{iex}$ values for an AS18

packed column and an AS18 coated 19 μm φ OT column were 118 and 8.6 μeq/mL, respectively, clearly indicating that much lower eluent concentrations are required to obtain essentially the same separation (bearing in mind that a linear relationship exists between log k and -log [E] and not k and [E], [E] being the eluent concentration.

### 3.3. Mass transfer in the microsuppressors. Is there laminar flow?

In any membrane-based ion exchange device, either mass transport *to* or *through* the membrane can ultimately limit the suppression capacity. However, whenever "quantitative" exchange is desired, as in a suppressor, and the device is operated to approach its maximum capacity, mass transport *to* the membrane must become the limiting process towards the end. Except for one early simulation [24], mass transport in suppressors have not been much studied. In Fig. 3, the SBC does increase from ~2 to 4.6 μS/cm linearly, with a slope of 94±6 nS/cm/mM KOH. Those familiar with suppressor behavior will recognize that this is not due to incomplete suppression; a very small amount of impurity, e.g., ~0.02% chloride relative to the KOH is sufficient to account for this degree of increase. At an SBC of <5 μS/cm, even as little as a change as 0.1 μS/cm is detectable. This change in conductance is equivalent to that due to 0.36 μM KOH. If this is the maximum unsuppressed amount in a 30 mM KOH eluent, the eluent is 99.999% suppressed. Mass transport to the wall for flow through a cylindrical conduit can be described by the first term approximation of the Gormley-Kennedy equation [25]:

$$1 - f = 0.819\exp(-3.657\mu) \quad (1)$$

where, $f$ is the fraction removed and $\mu$ is a dimensionless parameter equal to $\pi DL/Q$, $D$ being the diffusion coefficient of the transported species, $L$ being the length of the tube and $Q$ the flow rate. Using the diffusion coefficient of $K^+$ ($1.94 \times 10^{-5}$ $cm^2/s$), and a flow rate of 2.80 $\times 10^{-6}$ $cm^3/s$ (168 nL/min), only 99.7% removal is predicted for a 0.07 cm suppressor length according to Eq. 1. However, Eq. 1 pertains strictly to laminar flow conditions, which are the *least* conducive to efficient mass transfer to the wall. While the very small absolute flow rates in these μsuppressors may favor attainment of laminar flow, the abrupt diametric transitions at the entrance and exit of the device hinder the same. Although standard texts suggest a length of 0.05 $dN_{Re}$ where $d$ is the diameter of the tube and $N_{Re}$ is Reynold's number ($4Q\rho/(\pi d\eta)$, $\rho$ and $\eta$ being the density and viscosity of the fluid) is needed to attain 98% of the fully developed laminar flow pattern [26]; with present numerical values put in, this amounts to only 0.2 μm. However, given that mandrel-cast channels will not have perfectly smooth walls, especially relative to the diametric scale; this is also likely to inhibit development of perfectly laminar flow.

### 3.4. Chemical vs. electrodialytic suppression. Choice of regenerant

One motivating reason to pursue OTIC is facile field application, perhaps even in extraterrestrial exploration. In any field use, especially in space applications, simplicity, small footprint, and low power consumption are paramount. An electrodialytic suppressor can provide more capacity but is more complex in design with a necessarily larger power requirement and footprint, albeit admittedly not by a large margin. However, there are less things to fail in chemically regenerated suppressors, which are also known to stabilize more rapidly. Since limited number of samples are to be analyzed at a time, and in OTIC, the absolute amounts involved are very small (for 10 mM KOH eluent flowing at 150 nL/min, an 8-hour workday will consume < 1 μeq of eluent, requiring a proportionate amount of regenerant. To prolong the period before regenerant replacement is needed, obviously it will be preferable to use a higher regenerant concentration, assuming only a finite volume of regenerant can be carried on-board. The downside of a higher regenerant concentration is that Donnan-forbidden ion (or regenerant) penetration increases, increasing the background conductance and noise, and deteriorating sensitivity. To our knowledge, details of such regenerant penetration have been studied only once before, more than 3 decades ago [27]. These authors used an electrostatic model to predict that the forbidden regenerant flux through the membrane should increase as a quadratic function of the regenerant concentration; this was observed. In addition, as may be predicted, such penetration decreased dramatically with increasing size and charge of the regenerant counterion. In so far as membrane properties are concerned, the ionic site density (reciprocally related to the equivalent weight, EW) was the only factor considered , a higher charge density predictably decreases the penetration of similarly charged ions. Like other transmembrane fluxes, for a given concentration difference across the membrane, the flux is assumed to be linearly proportional to the membrane area and inversely as its thickness. With water flowing inside and 25 meq/L $H_2SO_4$ (a regenerant commonly used since the early days of membrane suppressors [28,29]) on the outside, different samples of Nafion (EW 1100, a polymer with a perfluoroether matrix) was found to exhibit a flux of 8-10 pequiv/(cm.min). A radiation grafted PTFE tube with an EW of 520 showed a flux of 3.0 pequiv/(cm.min); however, a radiation grafted poly(ethylvinyl acetate) tube of EW 570, showed a flux of 23.3 pequiv/(cm.min). Such behavior, a lower EW poly(ethylvinyl acetate) tube exhibiting so much greater penetration than a higher EW Nafion or a comparable EW radiation-grafted PTFE tube, could not be explained [27]. In comparison, the present polyvinyl alcohol-polystyrenesulfonate membrane, with a MW of ~800, exhibited a forbidden ion flux of ~400 pequiv/(cm.min) under the same test conditions, an order of magnitude greater than any of the above! Although the quadratic dependence on the regenerant concentration is observed as well (Fig. 4), these results indicate that aside from the ion exchange group density, the nature of the matrix polymer profoundly affects the overall transport and is particularly high for the very hydrophilic poly(vinyl alcohol) based present polymer that exhibits extremely high water absorption [16]. Sulfuric acid at significant concentrations cannot be used as regenerant with this membrane.

Acids with anions that are multiply charged like naphthalenetrisulfonate or large like dodecylbenzenesulfonate exhibit dramatically less penetration. But it was also observed early that a polymeric multiply charged ion like poly(styrenesulfonate) shows essentially zero detectable penetration [27]. Fortunately, this material is commercially available in highly purified form for this particular purpose and provides excellent results (Fig. 4).

### 3.5. Two-dimensional detection in the OT format

The Achilles heel of suppressed IC is poor and nonlinear response to weak acids. Indeed, very weak acids do not respond at all. In a review of the various approaches developed to measure all acids regardless of their $pK_a$, Karu et al. [30] concluded that demonstrably the best approach is to introduce a small amount of strong base and measure the conductivity again [31]. A methodically simpler variation of this technique, involving vapor phase introduction of the base through a nonionic membrane, was recently introduced [22]. Such two-dimensional conductometric detection can not only provide detection across the $pK_a$ horizon, it can provide $K_a$ and ionic mobility values and detect the presence of impurities. However, a potential pitfall common to all these techniques is the possible loss of neutrals (including un-ionized (very)weak acids) through the suppressor membrane. Shortly after the initial invention of IC [1] and the introduction of the nonsuppressed conductometric technique [32], Okada and Kuwamoto [33] pointed out that low concentrations of KOH provide excellent conditions for detection of very weak acids. Because of the low $\gamma_{iex}$ values, OT columns provide a unique opportunity to nonsuppressed admittance detection first, followed by a suppressor and suppressed detection.

Normally, connecting any external detector leads to an unacceptable

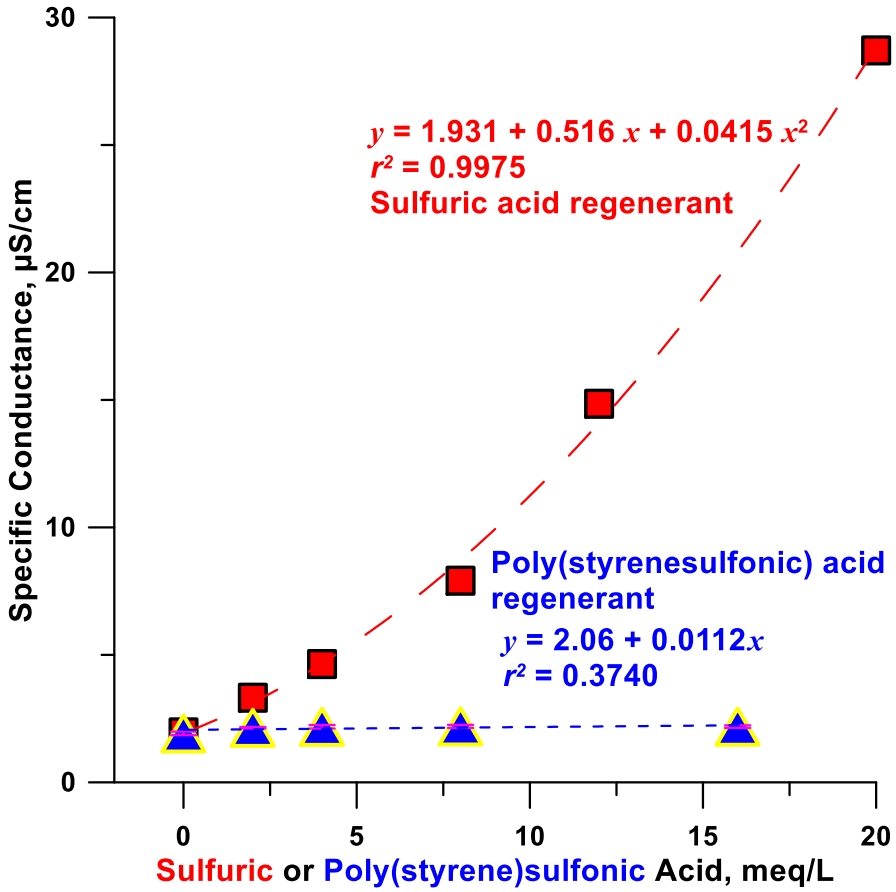


**Fig. 4.** Regenerant penetration, Sulfuric vs. poly(styrenesulfonic) acid. µSuppressor made on 50 µm wire mandrel (channel φ ~77 µm, active length 1.5 mm). DI water influent, 195 nL/min.

amount of dispersion. However, admittance (often inappropriately called contactless conductance [34]) detection is possible on-column and is widely used in capillary electrophoresis. Such on-column detection provides for almost no dispersion. On the other hand, it produces poor and nonlinear response in very small capillaries when the background conductance is low, as in suppressed OTIC. Operating at low probe frequencies may ameliorate the problem [35], but does not eliminate it [36]. A sequential on-column nonsuppressed admittance detector followed by a suppressor with an integrated true conductivity detection cell following it thus provides a uniquely applicable arrangement. In Fig. 5, we show the results of an arrangement that is far from optimized. Given the much higher background conductance of the nonsuppressed detector and the fact that no temperature stabilization was used (column and detector both were in ambient air), baseline noise is much higher. One may justifiably question whether new analytes that were not detectable in the suppressed detector can be detected under these circumstances at all. This question is clearly answered by the asterisked peaks in the nonsuppressed trace that are not visible in the suppressed trace. The second asterisked peak can be identified as $CO_2$ but the first peak, completely unanticipated, may in fact be due to sodium present in the analytes: recall that in all surface agglomerated columns, the underlying cation exchange sites are also accessible, in principle allowing for simultaneous cation-anion analysis. Further, the minor peaks, denoted by question marks (and showed in amplified form in the red trace), and quite possibly the shoulder on the nitrate peak, may well be other weak acid analytes whose presence can be confirmed with certainty only after further improvement in S/N is made. Note that in Fig. 5, not only the time scale has an offset between the top and bottom abscissae to account for the passage through the suppressor and the detector, the span is also longer in the suppressed chromatogram time scale to account for the additional column length.

*Prima Facie,* the two-dimensional detection approach, specifically the nonsuppressed detection, will not work with gradient elution. However, baseline rise in a gradient run occurs much more slowly (lower slope) than analyte peak excursion; given the progress that has been made in Fourier analysis of chromatographic data [37], or simply interpolating the baseline by numerical interpolation between peak valleys, baseline correction should be straightforward to implement.

### 3.6. *Suppressor-induced dispersion and column efficiency*

The data currently presented were all obtained with an automated commercial internal slot injector for convenience, the minimum injection volume was 4 nL. In a 25 µm φ column, this amounts to a length of ≳ 3 cm, ~6% of the length of the 51 cm column, much greater than what would provide optimum efficiency. But even under these conditions, it is possible to conclude that suppressor-induced dispersion is still perceptible: peak efficiencies decrease from the nonsuppressed to the suppressed detector, there is even a perceptible difference between the efficiencies observed with the 0.4 mm vs. the 0.7 mm suppressor (see Table 1). There is thus still a continued incentive to develop smaller bore suppressors, especially if the column bore is to be reduced further.

It is worth comparing the efficiencies reported in Table 1 with those calculated from the relevant form of the Golay equation [38,39] that does not account for any stationary phase mass transfer limitations (unlikely in a monolayer latex-based stationary phase, where individual latex particles are only 65 nm in diameter):

$$H = \frac{2D_m}{u} + \frac{1 + 6k + 11k^2}{24(1 + k)^2}\frac{r^2}{D_m}u \qquad (2)$$

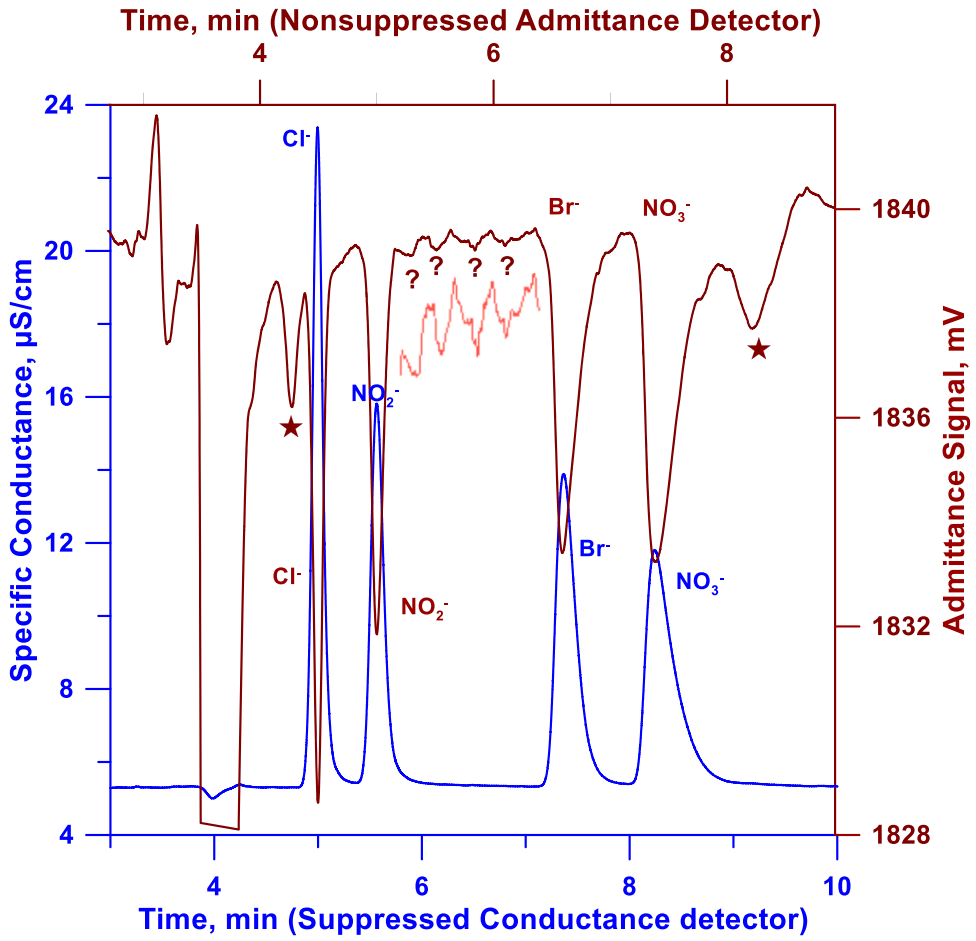


**Fig. 5.** Nonsuppressed admittance detection (dark red trace) before µsuppressor C (0.4 mm) and suppressed conductivity trace (blue). Note time axis origins are not the same in the top and bottom time axes. Abscissa span: bottom axis 3.00-10.00 min, top axis 2.70-8.925 min. PEEK column, 25 /360 µm, i.d./o.d.; Total length: 517 mm; Flow rate: 115 nL/min; 100 µM each analyte; Eluent: 4 mM KOH. Admittance excitation 650 kHz, conductivity excitation: 3 kHz; Sampling rate: 187 Hz.

**Table 1**
Theoretical and Experimental Efficiencies.

| Analyte | Ret Factor k | Efficiency kPlates/m (sd) | | | |
|---|---|---|---|---|---|
| | | Theoretical | Non-Suppressed | Suppressor 0.4 mm | Suppressor 0.7 mm |
| Chloride | 0.31 | 32.4 | 29.0 (2.4) | 22.1 (0.5) | 20.7 ($0.7_5$) |
| Nitrite | 0.46 | 24.7 | 23.4 (3.1) | 17.0 (0.5) | 15.2 (0.4) |
| Bromide | 0.92 | 17.9 | 13.3 (3.0) | 12.6 ($0.3_5$) | 11.6 (0.3) |
| Nitrate | 1.15 | 14.6 | 8.3 (0.3) | 8.3 (0.5) | 7.1 (0.2) |

where $H$, $D_m$, $u$, $k$, and $r$ respectively connotes plate height, diffusion coefficient of the analyte in the mobile phase, eluent linear velocity (0.404 cm/s for the data in Table 1), analyte retention factor and the radius of the capillary, respectively. $D_m$ was computed from the tabulated equivalent conductance data and the Nernst-Einstein equation. $D_m$ in $cm^2/s$ ranged from $1.89 \times 10^{-5}$ for $NO_3^-$ to $2.07 \times 10^{-5}$ for $Br^-$ [40]. It will be observed that except for nitrate, the experimental efficiency values for the nonsuppressed detection are not vastly different from theoretical (maximum) expectations. This is especially notable considering that the large injection volume is adversely affecting the early eluting peaks in particular. The experimental plate counts were computed based on 5.54 $(t_R/W_{0.5})^2$which implicitly assumes a Gaussian peak; this is clearly not the case for nitrate and may be part of the reason for the greater departure of the efficiency computed for nitrate from theoretical expectations. In addition, the difference from theoretically expected values seems to increase with increasing $k$. While we have neglected resistance to mass transfer in the stationary phase, this is inversely related to the diffusion coefficient in the stationary phase; this is expected to be smaller for high $k$ analytes. Finally, the difference in efficiency for nitrite in the nonsuppressed and the suppressed mode is not only due to dispersion in the suppressor but also the dependence of ionization and hence the conductivity signal on the concentration.

From Eq. 1 it can be readily computed that if operated at the optimum flow rates, the maximum efficiencies that should be attainable will range from ~62,800 plates/m for $NO_3^-$ to ~91500 for $Cl^-$, but those efficiencies will require corresponding flow rates of 0.01 – 0.04 cm/s, 40 - 10x lower than that used, resulting in impractically long separation times.

### 3.7. Low-level performance. Limits of detection

Fig. 6 shows the system response at sub-ppm levels (40 fmol, 1.4-3.2 pg injected) with two segments (2.0-3.0 min, 5.2 – 6.2 min) of the baseline shown magnified (right ordinate) as the blue traces. The drift-corrected baseline standard deviations are 1.2 and 1.1 nS/cm, respectively. One would appreciate that these values are respectable by commercial benchtop standards and especially remarkable in the absence of temperature stabilization. The signal/baseline standard deviation ratio for the chloride peak is ~900. On a S/N = 3 basis, the LODs for $Cl^-$, $NO_2^-$, $Br^-$, $NO_3^-$ are estimated to be 1.2, 3.8, 7.6, and 6.8 µg/L, respectively.

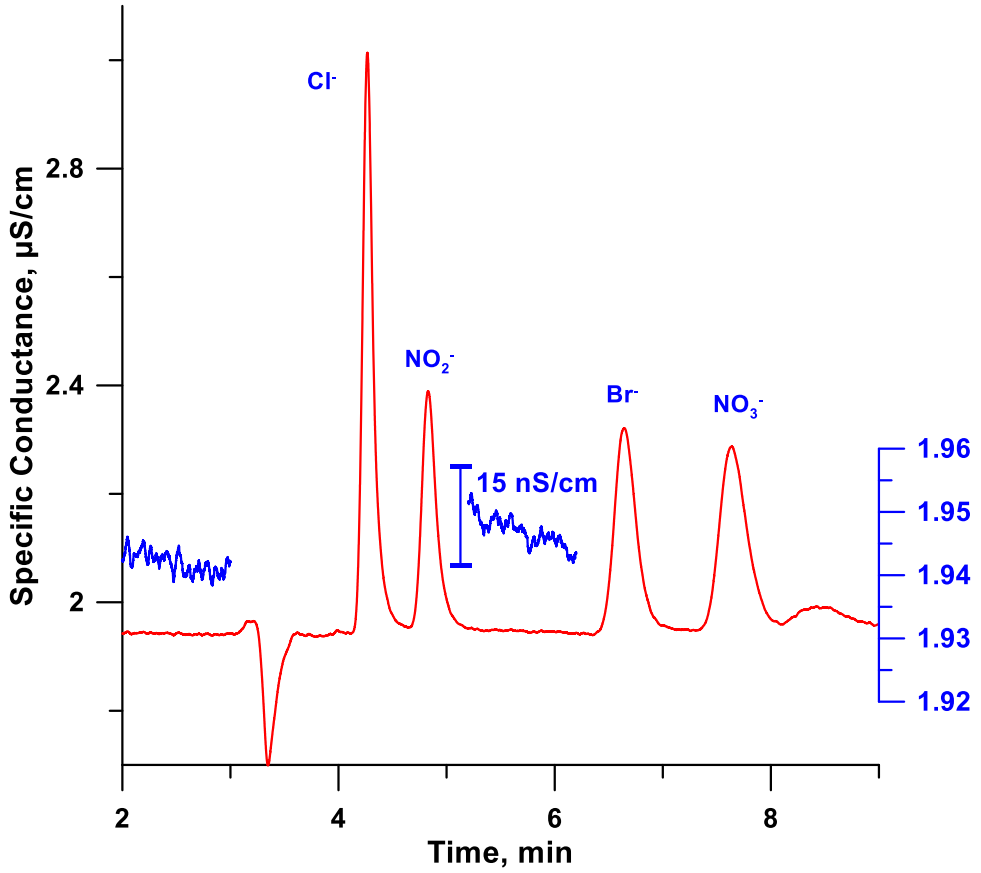


**Fig. 6.** Chromatogram at 10 µM analyte levels. Suppressor length 0.7 mm; conditions same as Figure 5 except flow rate is 126 nL/min.

## 4. Conclusions

We established a method to fabricate microsuppressors by casting a novel ion exchange polymer around a wire mandrel, crosslinking the material by thermal annealing, and subsequently removing the microwire. Despite a highly hydrophilic ion exchanger matrix, low background conductance chemical suppression and excellent detection performance was shown possible with an integrated tubular micro conductivity cell, with LODs for common ions in the single digit µg/L or single to double digit femtogram amounts injected on-column. The suppressor used in this work was ~45 µm in bore; although sub-mm in active length, the induced dispersion was perceptible. The next step will be to couple smaller bore columns and suppressors of matched bore.

## Author contributions

FM made the polymer, fabricated the suppressors and wrote the first version of the manuscript, BC fabricated columns and conductivity cells, did all the chromatography experiments, determined efficiencies and suppression capacities, CS did the MS experiments and generated the data in Figure S9, PKD conceived and directed the project, wrote the submitted and final revised version of the manuscript and created the majority of the graphics.

Supplementary materials

See supplementary materials for: Casting prepolymer around wire mandrel, test arrangement for measuring background conductance, mass spectral background for water and 0.01% HOAc direct and through suppressors, graphical and numerical data for MS ion count ratios at different flow rates for water and HOAc etc.

## Declaration of Competing Interests

The authors declare that they have no known competing financial interests or personal relationships that could have appeared to influence the work reported in this paper.

## Acknowledgment

This work was supported by NASA grant 80NSSC19K0805 through the MatISSE program, the National Science Foundation grant CHE-2003324, Thermo Fisher Scientific and the Hamish Small Chair endowment. We thank Chandan Choudhary for some of the photographs in Figure S1. Dr. Tobias Jonsson of Diduco AB, Sweden, is thanked for the gift of the purified poly(styrenesulfonic) acid.

## Supplementary materials

Supplementary material associated with this article can be found, in the online version, at doi:10.1016/j.talo.2021.100062.

## References

[1] H. Small, T.S. Stevens, W. Bauman, Novel ion exchange chromatographic method using conductimetric detection, Anal. Chem. 47 (1975) 1801–1809.
[2] P.K. Dasgupta, F. Maleki, Ion exchange membranes in ion chromatography and related applications, Talanta 204 (2019) 89–137.
[3] K. Srinivasan, B.K. Omphroy, R. Lin, C.A. Pohl, A new suppressor design for low noise performance with carbonate eluents for ion chromatography, Talanta 188 (2018) 152–160.
[4] S. Rokushika, Y.Q. Zong, L.S. Zhuo, H. Hatano, Microbore packed-column anion chromatography using a UV detector, J. Chromatogr. A. 280 (1983) 69–76.
[5] A. Sjögren, C.B. Boring, P.K. Dasgupta, J.N. Alexander, IV, capillary ion chromatography with on-line high-pressure electrodialytic NaOH eluent production and gradient generation, Anal. Chem. 69 (1997) 1385–1391.

[6] C.B. Boring, P.K. Dasgupta, A. Sjögren, A compact field portable capillary ion chromatograph, J. Chromatogr. 804 (1998) 45–54.
[7] P. Kuban, P.K. Dasgupta, Capillary ion chromatography. A review, J. Sep. Sci. 27 (2004) 1441–1457.
[8] A. Sedyohutomo, L.W. Lim, T. Takeuchi, Development of packed-column suppressor system for capillary ion chromatography and its application to environmental waters, J. Chromatogr. A 1203 (2008) 239–242.
[9] W. Huang, Open tubular ion chromatography: a state-of-the-art review, Anal. Chim. Acta 1143 (2021) 210–224.
[10] W. Huang, A. Plistil, S. Stearns, P.K. Dasgupta, Gradient Nanopump based suppressed ion chromatography using PEEK open tubular columns, Talanta Open 3 (2021), 100029.
[11] P. Kuban, P.K. Dasgupta, C.A. Pohl, Open tubular anion exchange chromatography. controlled layered architecture of stationary phase by successive condensation polymerization, Anal. Chem. 79 (2007) 5462–5467.
[12] X.J. Huang, P.K. Dasgupta, Controlled porosity monolithic material as permselective ion exchange membranes, Anal. Chim. Acta 689 (2011) 155–159.
[13] X.J. Huang, F. Foss, P.K. Dasgupta, Multilayer chitosan-based open tubular capillary anion exchange column with integrated monolithic capillary suppressor, Anal. Chim. Acta 707 (2011) 210–217.
[14] W. Huang, P.K. Dasgupta, K P., Electrodialytic capillary suppressor for open tubular ion chromatography, Anal. Chem. 88 (2016) 12021–12027.
[15] B. Chouhan, C.P. Shelor, W. Huang, Y. Chen, P.K. Dasgupta, Nanovolume gas-free hydroxide eluent generator for open tubular ion chromatography, Anal. Chem. 92 (2020) 5561–5568.
[16] F. Maleki, P.K. Dasgupta, Anal. Chem. 92 (2020) 13378–13386.
[17] D. Qi, T. Okada, P.K. Dasgupta, Direct current conductivity detection in ion chromatography, Anal. Chem. 61 (1989) 1383–1387.
[18] S. Tan, A. Laforgue, D. Bélanger, Characterization of a cation-exchange/polyaniline composite membrane, Langmuir 19 (2003) 744–751.
[19] A. Kraytsberg, Y. Ein-Eli, Review of advanced materials for proton exchange membrane fuel cells, Fuels 28 (2014) 7303–7330.
[20] A. Kusoglu, A.Z. Weber, New insights into perfluorinated sulfonic-acid ionomers, Chem. Rev. 117 (2017) 987–1104.
[21] K.D. Kreuer, Ion conducting membranes for fuel cells and other electrochemical devices, Chem. Mater. 26 (2013) 361–380.
[22] H. Liao, P.K. Dasgupta, Permeative amine introduction for very weak acid detection in ion chromatography, Anal. Chem. 88 (2016) 2198–2204.
[23] W. Huang, C.A. Pohl, P.K. Dasgupta, Ion exchange column capacities. predicting retention behavior of open tubular columns coated with the same phase, J. Chromatogr. A 1550 (2018) 75–79.
[24] P.K. Dasgupta, K P., Linear and helical flow in a perfluorosulfonate membrane of annular geometry as a continuous cation exchanger, Anal. Chem. 56 (1984) 96–103.
[25] P.G. Gormley, M. Kennedy, Diffusion from a stream flowing through a cylindrical tube, Proc. R. lr. Acad., Sect. A 52 (1949) 163–169.
[26] W. McKays, M.E. Crawford, Convective Heat and Mass Transfer, 2nd ed., McGraw-Hill, New York, 1980, pp. 66–68.
[27] P.K. Dasgupta, R.Q. Bligh, Q. R., J. Lee, V. D'Agostino, Ion penetration through tubular ion exchange membranes, Anal. Chem. 57 (1985) 253–257.
[28] T.S. Stevens, J.C. Davis, H. Small, Hollow fiber ion-exchange suppressor for ion chromatography, Anal. Chem. 53 (1981) 1488–1492.
[29] T.S. Stevens, G.L. Jewett, R.A. Bredeweg, Packed hollow fiber suppressors for ion chromatography, Anal. Chem. 54 (1982) 1206–1208.
[30] N. Karu, G.W. Dicinoski, P.R. Haddad, R P., Use of suppressors for signal enhancement of weakly-acidic analytes in ion chromatography with universal detection methods, TrAC Trends Anal. Chem. 40 (2012) 119–132.
[31] R. Al-Horr, P.K. Dasgupta, R.L. Adams, Two-dimensional detection in ion chromatography: sequential conductometry after suppression and passive hydroxide introduction, Anal. Chem. 73 (2001) 4694–4703.
[32] D.T. Gjerde, J.S. Fritz, G. Schmuckler, G. Anion chromatography with low-conductivity eluents, J. Chromatogr. A 186 (1979) 509–519.
[33] T. Okada, T. Kuwamoto, Potassium hydroxide eluent for nonsuppressed anion chromatography of cyanide, sulfide, arsenite, and other weak acids, Anal. Chem. 57 (2001) 829–833.
[34] M. Zhang, P. K. Dasgupta, Conductance or Admittance? Q&More Issue 215, October 2015. http://q-more.chemeurope.com/q-more-articles/215/conductance-or-admittance.html.
[35] M. Zhang, B.N. Stamos, P.K. Dasgupta, Admittance detection in high impedance systems. Design and applications, Anal. Chem. 86 (2014) 11547–11553.
[36] W. Huang, B. Chouhan, P.K. Dasgupta, Capillary scale admittance and conductance detection, Anal. Chem. 90 (2018) 14561–14568.
[37] A.F. Kadjo, P.K. Dasgupta, C.P. Shelor, Optimum cell pathlength or volume for absorbance detection in liquid chromatography. Transforming longer cell results to virtual shorter cells, Anal. Chem. 92 (2000) 6391–6400.
[38] M.J.E. Golay, Height equivalent to a theoretical plate of an open tubular column lined with a porous layer, Anal. Chem. 40 (1968) 382–384.
[39] L.M. Blumberg, Extension of Golay plate height equation for open-tubular columns, J. Chromatogr. A 1524 (2017) 303–306.
[40] G.D. Christian, P.K. Dasgupta, K.A. Schug, Analytical Chemistry, 7th Ed., Wiley, 2014, pp. 678–679. Ch 21.